

# Two-dimensional model of intrinsic magnetic flux losses in helical flux compression generators

V. V. Haurylavets\*, V. V. Tikhomirov†

September 26, 2012

Research Institute for Nuclear Problems, Belarusian State University,  
Bobruiskaya 11, 220030 Minsk, Belarus

## Abstract

Helical Flux Compression Generators (HFCG) are used for generation of mega-ampere current and high magnetic fields. We propose the two dimensional HFCG filament model based on the new description of the stator and armature contact point. The model developed enables one to quantitatively describe the intrinsic magnetic flux losses and predict the results of experiments with various types of HFCGs. We present the effective resistance calculations based on the non-linear magnetic diffusion effect describing HFCG performance under the strong conductor heating by currents.

## 1 Introduction

Helical flux compression generators (HFCGs) are compact pulsed power sources of current and voltage. The interest in HFCG studies primarily stems from their unique capability to achieve very high energy densities, magnetic field strengths and to generate high-power current pulses. They find promising applications in particle accelerator technology, magnetic plasma confinement, neutron radiation pulse and Z-pinch generation, as well as in thermonuclear research. In this field, they are a relatively cheap option to large stationary mega-ampere pulsed current generators. There is an interesting proposal to use HFCGs with nuclear explosives for developing accelerators having a short operating time and a very large beam luminosity at the energies only recently available in modern accelerators. Moreover, based on HFCG, it is possible to create a large pulsed magnetic lens for focusing proton beams of intensity  $10^{23}$  protons per second per surface area of about  $1 \text{ mm}^2$  [1].

The idea of the FCG was first proposed and substantiated in 1951 by A. D. Sakharov [1], who suggested converting the chemical energy of explosives into magnetic field energy. His suggestions were implemented in 1952 in the MK-1

---

\*E-mail:bycel@tut.by

†E-mail:vvtikh@mail.ru

experiments on magnetic flux compression performed in VNIIEF (Russian Federal Nuclear Center All-Russia Research Institute of Experimental Physics). In 1952, M. Fowler in the United States compressed the magnetic field using his first plate generator [11]. Many countries have joined in the research on FCGs ever since.

Some difficulties were encountered in theoretical description of the HFCG. Theoretically predicted currents were several times as large as those measured experimentally [8].

Various empirical factors affecting the magnetic flux losses were used to eliminate the discrepancies between theoretical estimates and experimental data. As a rule, these factors were not of universal character, and thus applied to certain HFCG designs or operation parameters. For example, the resistance could be increased by a factor of two and more, depending on the HFCG design, the load used, and the initial current. A number of HFCG numerical models using these factors have been proposed over the years. The awareness of the fact that besides the resistance losses, there exist other losses in the vicinity of the contact point appeared to be the only consistent view [7, 8, 10].

The numerical model suggested in the present paper enables describing the parameters of operating HFCGs. It is shown that because of the lack of comprehension about the nature and effects of magnetic flux losses, some of them were neglected earlier. The developed numerical model of the HFCG moving contact point gives the insight into the nature of these losses and allows computing their values.

## 2 Geometry and Operating Principle

HFCG is a device compressing a magnetic flux. The magnetic flux  $\Phi$  passing through the surface  $S$  can be found using the surface integral:

$$\Phi = \int_S \mathbf{B} \cdot d\mathbf{s}, \quad (1)$$

where  $B$  is the magnetic field induction, and if the closed circuit  $c$  belongs to the open surface  $S$ , then [13]:

$$\frac{d\Phi}{dt} = -\frac{d}{dt} \int_S \mathbf{B} \cdot d\mathbf{s} = \oint_c \mathbf{E} \cdot d\mathbf{l}, \quad (2)$$

where  $\mathbf{E}$  is the electric field strength along the closed circuit  $c$ ,  $\mathbf{E} \cdot d\mathbf{l}$  shows that here the differential length  $d\mathbf{l}$  the electric field tangential with respect to the circuit are used. One can see from (2) that with the conserved magnetic flux and decreasing length of the conducting closed circuit  $c$ , both the electric field and the current increase in the circuit. By definition, the inductance of the closed circuit

having a current  $I$  is

$$L = \frac{\Phi}{I}, \quad (3)$$

The physical principle governing the operation of the HFCG is based on Faraday's law.

$$\frac{d\Phi}{dt} = -RI, \quad (4)$$

where  $\Phi$  is the magnetic flux in the HFCG,  $R$  is the resistance, and  $I$  is the current.

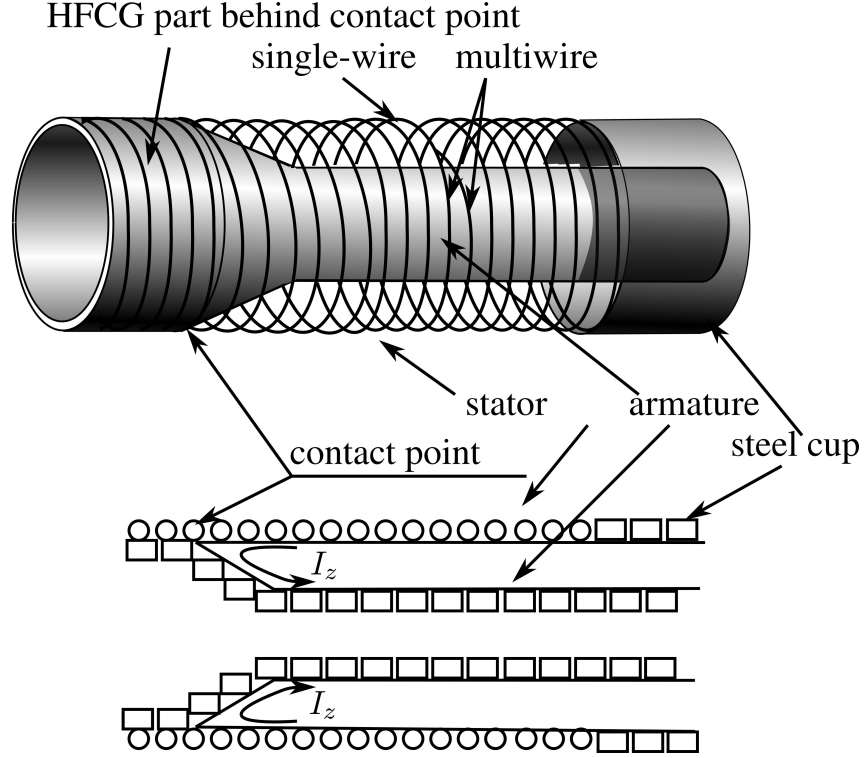


Figure 1: Main parts of the HFCG. Sectional view

The HFCG design is illustrated in Fig. 1; its main parts are the solenoid, called the stator, and the metal tube, called the armature. The stator with a single-wire coil is called the single-wire stator; a plural number of metal wires helically wound together and arranged in parallel relation with each other form a multi-wire stator; the number of winds corresponds to the number of wires wound in parallel. The armature, made of copper or aluminium, is placed inside the stator and is filled with explosives. Cups, conducting tubes having the same radius as the radius of the stator, are often used in HFCG design: placed at the head, they reduce the effect of the armature and stator closure on the HFCG performance, placed at the back, they provide the current output to the load. The armature and the stator are switched into the circuit and connected through the load, as shown in Fig. 2.

The external magnetic field or the initial current in the stator are used to produce a magnetic flux. The explosives are ignited from the head of the armature,

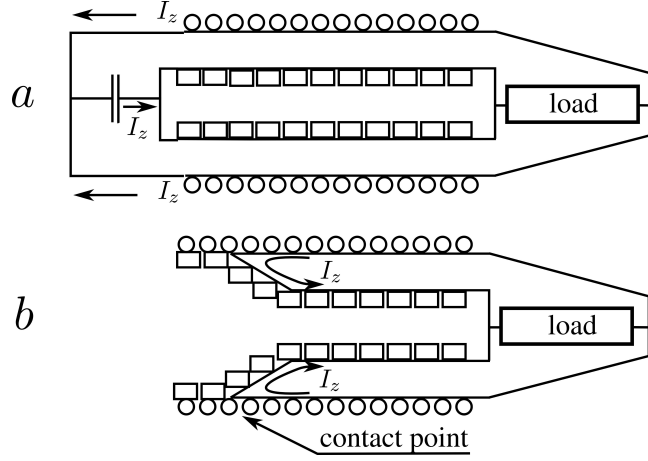


Figure 2: Stages of HFCG operation: *a* is establish initial current, *b* is magnetic flux compression

forcing it to expand. The expanding armature, forming a conical plane moving along the length of the generator, reaches the stator and sequentially shorts out the turns of the stator.

### 3 Review of the Methods for HFCG Description

Let us consider the main approaches to the description of HFCG operation. In view of (4), we have

$$I \frac{dL}{dt} + L \frac{dI}{dt} + RI = 0. \quad (5)$$

The solution to (5) is

$$I = I_0 \frac{L_0}{L} e^{-\int \frac{R}{L} dt}. \quad (6)$$

All electrotechnical models, as a rule, can be reduced to equation (5), though the methods used to calculate the inductance or the resistance may vary. But the models based on the solution of the equations of magnetohydrodynamics are fundamentally different. The models based on (5) are called zero-dimensional (0D) when the inductance and resistance are defined by certain functions of time, and one-dimensional (1D) when the inductance and the resistance are certain functions of the coordinates along the HFCG axis and are calculated at every integration step.

A two-dimensional HFCG model was suggested in [6] and described in [2]. The current-carrying elements of the HFCG are decomposed as shown in Fig. 3 (see [6]). The helical FCG is decomposed into equivalent  $z$ - and  $\theta$  current-carrying circuits. The stator-armature-load electric circuit consists of a coaxial part and  $z$ -circuits connected to the load.

The stator is decomposed into  $N$  number of rings equal to the number of the solenoid turns, through which the load current flows in the azimuthal direction,

inducing the axial magnetic field  $B_z^z$ ; the coaxial part of the generator produces the field  $B_\theta$ . To correctly describe the  $\theta$ -current in the armature, which is induced by a changing current  $I_z$  in the stator, let us consider several separate  $\theta$  circuits taken as separate rings equal in number to the number of the solenoid turns,  $N$ , as shown in Fig. 3, and arranged in the equivalent electric circuit as shown in Fig. 4). The current  $I_i^\theta$  induces the axial magnetic field  $B_z^\theta$ .

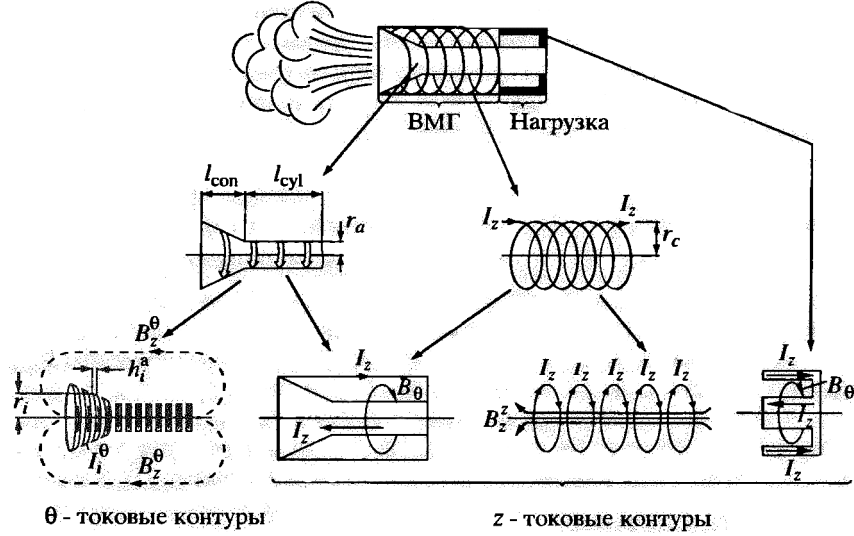


Figure 3: Schematic diagram of HFCG analysis. Decomposition of the stator and the armature into  $\theta$  and  $z$  current-carrying circuits

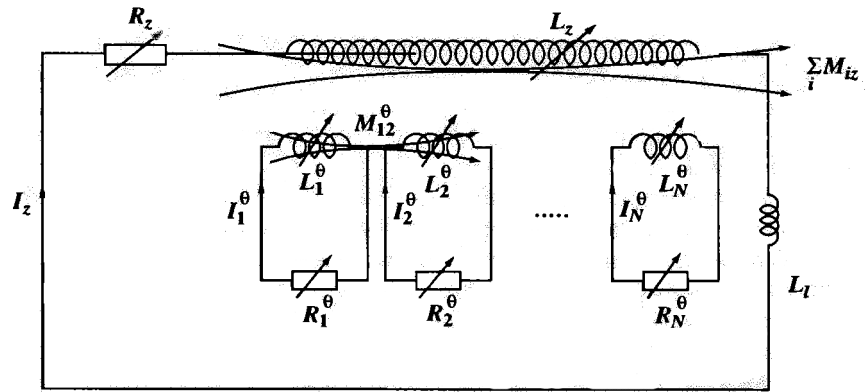


Figure 4: Equivalent electric circuit for  $\theta$  and  $z$  current-carrying circuits.

The system of equations given in [6] for the decomposed circuits has the form (7) and (9).

For the load circuit

$$L_z \frac{dI_z}{dt} + \sum_{i=1}^N \left( M_{iz} \frac{dI_i^\theta}{dt} + I_i^\theta \frac{dM_{zi}}{dt} \right) + \left( R_z + \frac{dL_z}{dt} \right) I_z = 0, \quad (7)$$

where  $L_z$  is the stator inductance,  $M_{iz}$  is the mutual inductance between the  $i$ -th ring of the armature and the stator, and  $I_i^\theta$  is the current in the  $i$ -th ring of the armature.

$$R_z = R_z^l + R_z^z + R_z^p + R_{load}, \quad (8)$$

where  $R_z^l$  is the resistance of the armature to current  $I_z$ ,  $R_z^z$  is the resistance of the stator,  $R_z^p$  is the resistance describing the proximity effect, which is allowed for when the diameter of the stator wire is less than the coil pitch because of the insulation, and  $R_{load}$  is the resistance of the load.

For  $\theta$ -circuits, we write  $N$  number of equations:

$$L_i^\theta \frac{dI_i^\theta}{dt} + M_{iz} \frac{dI_z}{dt} + I_z \frac{dM_{iz}}{dt} + \sum_{j=1(j \neq i)}^N \left( M_{ij}^\theta \frac{dI_j^\theta}{dt} + I_j^\theta \frac{dM_{ij}^\theta}{dt} \right) + \left( R_i^\theta + \frac{dL_i^\theta}{dt} \right) I_i^\theta = 0, \quad (9)$$

where  $i = 1, 2, 3, \dots, N$  is the number of  $\theta$ -circuits,  $L_i^\theta$  is the inductance of the  $i$ -th ring of the armature,  $M_{ij}^\theta$  is the mutual inductance of the armature rings, and  $R_i^\theta$  is the resistance of the  $i$ -th ring of the armature.

For a better understanding of equations (7) and (9), let us represent them in a compact form:

$$\frac{d}{dt} \left( L_z I_z + \sum_{j=1}^N M_{j,z}^\theta I_j^\theta \right) = -R_z I_z \quad (10)$$

and

$$\frac{d}{dt} \left( M_{i,z}^\theta I_z + \sum_{j=1}^N M_{i,j}^\theta I_j^\theta \right) = -R_i^\theta I_i^\theta, \quad i = 1 \dots N, \quad (11)$$

where  $M_{i,i}^\theta = L_i^\theta$  is the self-inductance of the  $i$ -th ring if  $j = i$ .

B.M. Novac et al. [6] have considered the problem of the stator turns switching off after the closure of the armature. In this model, the number of stator turns is the same as the number of the armature rings. When the stator turn is closed, the opposite-lying armature ring is eliminated from the system of equations (7) and (9). The currents in the circuits are recomputed so that the magnetic fluxes before and after the elimination of the turn and the armature ring will be equal.

An interesting model for magnetic flux loss simulation was developed by Kiuttu and co-workers in [8, 9], where the magnetic field diffusion into the conductor was considered. By approximating the nonlinear magnetic diffusion and comparing it with the flux compression rate one can identify some distinct regions in the vicinity of the moving contact point, which are separated by the critical and transition points. At the critical point, the rate at which the magnetic flux is pushed ahead by the expanding armature is almost equal to the rate of flux diffusion into the conductor, and so the magnetic flux after the critical point is

wasted for compression. Transition point is the point behind which the stator turn-armature proximity effects are more important than the turn-to-turn effects. These effects lead to arising effective resistance as described by Kuittu. This approach seems promising because it allows taking account of the magnetic flux loss at the contact point for magnetohydrodynamical, 0D, and 1D models. The resistance at the contact point, as defined by Kuittu, is derived from theoretical considerations and enables one to describe specific HFCGs, but it does not agree with the conclusions and computations made in [7].

The idea suggested and substantiated in [7] is that the magnetic flux losses are concentrated in the vicinity of the moving contact point and are not related to resistance, as only taking this approach, one can simultaneously match both the output voltage and the current of the HFCG with its parameters. The authors of [7] propose to describe the magnetic flux loss, called the intrinsic loss, using the following equation for the HFCG:

$$I \cdot \alpha \cdot \frac{dL}{dt} + L \frac{dI}{dt} + IR = 0, \quad (12)$$

where  $\alpha$  is the flux loss parameter, varying within the interval from 0 to 1. It is also stated that though the flux losses cannot currently be computed numerically, one can approximate them by the flux loss parameter  $\alpha$  and that the losses occur only after the appearance of the moving contact point between the stator and the armature. In the present paper, a different approach is applied to the consideration of magnetic flux losses. Using this approach, one can with satisfactory accuracy describe HFCGs of completely different designs and with various stators on the basis of the physical theory and pre-experimental data alone, and thus predict the results of the experiments.

## 4 Basic Formulas. Governing Equations

In the present paper, a two-dimensional model of the HFCG, based on the model described in [6], is developed. For correct computation of the current distribution in the armature, we used the following decomposition: the stator is decomposed into the turns and the armature is decomposed into the rings, which are assigned the equivalent current-carrying circuits (see Fig.5). Each equivalent circuit is assigned the self-inductance  $L_i = M_{ii}$  and the resistance  $R_i$ . In this case, the system of equations for equivalent circuits takes the form:

$$\sum_j^n M_{ij} \frac{dI_j}{dt} + \sum_j^n \frac{dM_{ij}}{dt} I_j + R_i I_i = U_i, \quad (13)$$

where  $U_i$  is the voltage produced in the circuit as a part of the electric circuit (galvanic coupling between the turns of the stator), and  $M_{ij}$  is the mutual inductance between the equivalent circuits  $i$  and  $j$ ; here  $i, j = 1 \dots n$ , where  $n$  is the

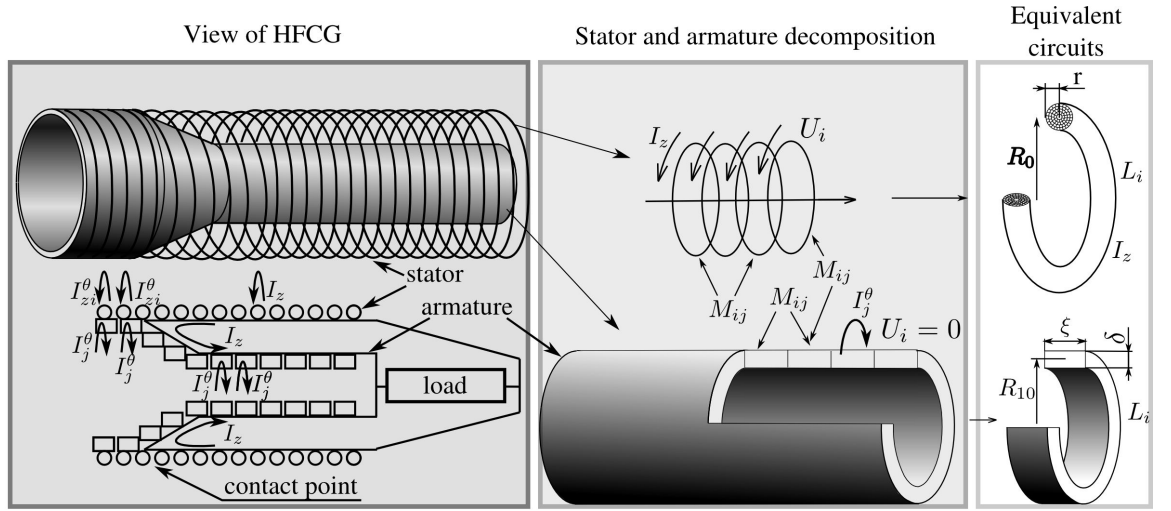


Figure 5: Decomposition of the HFCG elements into the equivalent current-carrying circuits,  $I_z$  is the current in the stator-armature-load electric circuit,  $I_j^\theta$  is the current in the armature rings,  $I_{zi}^\theta$  are the  $\theta$ -currents in the stator turns after it has contacted the armature and has been eliminated from the stator-armature-load electric circuit

total number of the current-carrying circuits. In solving the system of equations (13), we assume that the rings of the armature and the metal cup are not connected with zero voltage across them. The voltage across the load equals the total voltage of the stator turns

$$\sum_{i=k+1}^N U_i = U_{load}, \quad (14)$$

where  $k$  is the number of the stator turns switched out of the electric circuit and at the initial time,  $k$  equals zero. The voltage  $U_i$  across the turns switched out of the electric circuits is zero.

To solve the system of equations (13), let us recast it in the form:

$$\begin{aligned} M_{11} \frac{dI_1}{dt} + M_{12} \frac{dI_2}{dt} + \dots &= -\frac{dM_{11}}{dt} I_1 - \frac{dM_{12}}{dt} I_2 - \dots - R_1 I_1 + U_1 \\ M_{21} \frac{dI_1}{dt} + M_{22} \frac{dI_2}{dt} + \dots &= -\frac{dM_{21}}{dt} I_1 - \frac{dM_{22}}{dt} I_2 - \dots - R_2 I_2 + U_2. \end{aligned} \quad (15)$$

.....

The dependent variables are canceled out; in the elements outside the electric circuit, the unknown quantities  $U_i$  are either switched out or equated to zero:

$$\begin{aligned} L_z \frac{dI_z}{dt} + M_{z,N+1} \frac{dI_{N+1}}{dt} + \dots &= -\sum_{i=1}^N \frac{dM_{i1}}{dt} I_1 - \sum_{i=1}^N \frac{dM_{i2}}{dt} I_2 - \dots - R_z I_z \\ M_{z,N+1} \frac{dI_z}{dt} + M_{N+1,N+1} \frac{dI_{N+1}}{dt} + \dots &= -\frac{dM_{N+1,1}}{dt} I_1 - \frac{dM_{N+1,2}}{dt} I_2 - \dots - R_{N+1} I_{N+1}, \end{aligned} \quad (16)$$

where  $L_z = \sum_{i=1}^N M_{ii}$ ,  $M_{zi} = \sum_{j=1}^N M_{ji}$ , and  $R_z = \sum_{i=1}^N R_i$  are the quantities characterizing the stator included into the stator-armature-load electric circuit,  $L_z$  is the stator inductance,  $M_{iz}$  is the mutual inductance between the  $i$ -th circuit of the armature ring and the stator, and  $R_z^z$  is the resistance of the stator. We



thus obtain the system of rank  $n - N + k + 1$ , where  $N$  is the number of the stator turns; for  $k = 0$  (all the stator turns are included into the electric circuit), the system has rank  $n - N + 1$ , with  $n$  being the number of HFCCG current-carrying circuits. When the first stator turn is switched out of the electric circuit, and  $k = 1$ :

$$\begin{aligned}
M_{1,1} \frac{dI_1}{dt} + M_{z,1} \frac{dI_z}{dt} + M_{1,N+1} \frac{dI_{N+1}}{dt} + \dots &= -\frac{dM_{1,1}}{dt} I_1 - \frac{dM_{1,2}}{dt} I_2 - \dots - R_1 I_1 \\
M_{2,1} \frac{dI_1}{dt} + L_z \frac{dI_z}{dt} + M_{z,N+1} \frac{dI_{N+1}}{dt} + \dots &= -\sum_{i=2}^N \frac{dM_{i1}}{dt} I_i - \dots - R_z I_z \\
M_{N+1,1} \frac{dI_1}{dt} + M_{z,N+1} \frac{dI_z}{dt} + M_{N+1,N+1} \frac{dI_{N+1}}{dt} + \dots &= -\frac{dM_{N+1,1}}{dt} I_1 - \dots - R_{N+1} I_{N+1}. \\
&\dots\dots\dots
\end{aligned} \tag{17}$$

To take account of the load in the electric circuit and the coaxial part of the HFCCG, let us add the inductance of the load ( $L_{load} = const$ ) and the inductance of both the armature and the metal cup ( $L_{line}^z$ ) to the inductance of the stator; we shall also add the resistance of the load ( $R_{load}$ ) and the armature and the metal cup ( $R_{line}$ ) to current  $I_z$  to that of the stator. Then the system of equations takes the form:

$$\begin{aligned}
&(L_z + L_{load} + L_{line}^z) \frac{dI_z}{dt} + M_{z,N+1} \frac{dI_{N+1}}{dt} + \dots = \\
&= -\frac{dL_{line}^z}{dt} I_z - \sum_{i=1}^N \frac{dM_{i1}}{dt} I_i - \sum_{i=1}^N \frac{dM_{i2}}{dt} I_2 - \dots - (R_z + R_{line} + R_{load}) I_z \\
M_{z,N+1} \frac{dI_z}{dt} + M_{N+1,N+1} \frac{dI_{N+1}}{dt} + \dots &= -\frac{dM_{N+1,1}}{dt} I_1 - \frac{dM_{N+1,2}}{dt} I_2 - \dots - R_{N+1} I_{N+1}. \\
&\dots\dots\dots
\end{aligned} \tag{18}$$

From (18) we find the derivative of current for each of the circuits and restore the currents in the circuits using Euler's method:

$$I_i = I_i^0 + h * \frac{dI_i}{dt}, \tag{19}$$

where  $h$  is the time step. The Euler method is applied twice: The resistance is computed for each current-carrying circuit and then the current is computed for each circuit. The average resistance of each circuit during the time step is computed and then the current in each circuit is re-computed.

The main differences of the model proposed here from that described in [6] are as follows:

- The armature is decomposed into a substantially larger number of rings than the number of rings in the stator;
- Account is taken of the arbitrary geometric dimensions of the stator and the metal cups on the HFCCG ends;
- The part of the HFCCG behind the contact point is modeled instead of being ignored;

- The stator turn at the contact point is decomposed into smaller parts to achieve higher accuracy of modeling;
- The developed model naturally takes into account the intrinsic flux losses;

It should be noted that for the described two-dimensional model, the term  $\frac{dL_z}{dt}$  in (7) can be put equal to zero in the case when in HFCG modeling neither the stator rings are displaced nor their radii are changed. In the considered model this occurs spontaneously, since the circuit eliminated from the electric circuit remains there as a free current-carrying circuit. This is basically different from the model proposed by Novac and co-authors [6], where the elimination problem leads to a nonzero value of the term  $\frac{dL_z}{dt}$  because the current is deliberately eliminated from the closed turns of the stator, while the associated magnetic flux is artificially re-distributed.

## 5 The Moving Contact Point Model and the Intrinsic Flux Losses in the HFCG

The region of the moving contact point was modeled in [7]. The obtained result showed that the current changed direction after passing the contact point, flowing from the stator into the armature. Let us check the result against the model of the HFCG as a whole.

Let us project the current on the HFCG axis. This gives us the coaxial part of the HFCG. Let us now project the currents on the plane perpendicular to the axis. The projections of the currents coincide with the currents flowing in the equivalent circuits after the decomposition of the HFCG conducting elements (Fig.5).

As is seen in Fig. 5, the stator turns are closed through the armature behind the contact point, and hence  $\theta$ -currents may flow through the turns. In terms of magnetic diffusion, we have two circular rings with adjacent surfaces, through which the opposite currents flow. The characteristic time for the observed skin depth of  $2 \cdot 10^{-4}$  m is from 1 to 10 microseconds. The same or longer time is required for current compensation, which is comparable to the HFCG operating time. Thus, the idea of a rapid current attenuation behind the contact point does not describe a real physical picture of HFCG operation. The idea of slow current attenuation is confirmed by indirect simulation of HFCG using (13) and computing the current density distribution over the HFCG conductors [12]. At the moment of the turn closure, the current in the turn is the same as the current in the stator and is further calculated by the system of equations (13). The armature ring stops after it has contacted the stator, and does not move until the computations are over, so the closed stator turn is switched out of the stator-

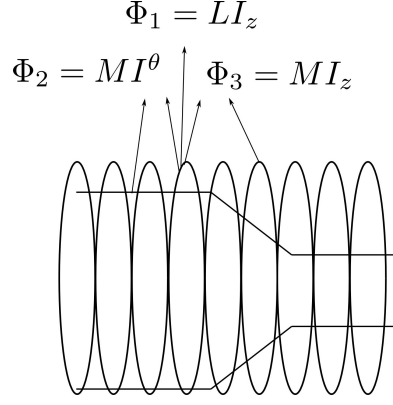


Figure 6: Intrinsic flux loss, the lost magnetic flux

armature-load electric circuit. In the model presented here the closed turn of the stator is considered as an independent circuit connected to the rest of the circuits via the magnetic field. The sum of the mutual magnetic flux of the closed stator turn and the opposite armature rings of the HFCG behind the contact point is much smaller than the intrinsic magnetic flux of the stator turn or the armature ring. Hence, the assumption that the armature ring and the stator turn are fixed after the closure does not significantly affect the results of computation.

When the stator turn is closed and switched out of the stator-armature-load electric circuit, the magnetic flux linked to it is lost, which includes the flux of the turn itself and the fluxes of other turns of the stator and of the armature rings. What remains is the mutual flux between the switched turn and the operating part of the stator (Fig. 6). Thus, for calculating the losses, one needs to consider the flux of the stator and the armature behind the contact point. For HFCGs with superconducting generators, this sum flux is equal to zero. In a real HFCG, the stator turns and the armature rings have different current densities, as well as the ohmic losses, and so the magnetic flux in the HFCG behind the contact point is larger the larger is the difference between the losses in the stator and the armature. In the model described in [6], the magnetic flux is artificially redistributed from the closed turns of the stator into the HFCG part in front of the contact point, leading to an erroneous representation of the current distribution over the armature and disregard of the intrinsic flux loss.

## 6 One-Dimensional Model with Regard for the Intrinsic Flux Loss

Let us distinguish the magnetic flux  $L_z$  in the stator conductor. Recast (5) as

$$I \frac{dL}{dt} + L \frac{dI}{dt} + RI + \frac{dL_z}{dt} I = 0, \quad (20)$$

which includes the flux taken away by the turns. The solution of (20) for HFCG current has the form:

$$I = I_0 \frac{L_0}{L} e^{-\int \frac{R}{L} dt - \int \frac{dL_z}{dt} \frac{1}{L} dt}. \quad (21)$$

## 7 Inductance

For a two-dimensional model, one needs to calculate both the self-inductances of equivalent circuits and the mutual inductances between them. Equivalent circuits are presented as circular loops with geometrical mean distance  $g_i$  between the area of the wire cross section and itself [3]. In this case, the inductance of each circuit is defined by:

$$L = \mu_0 R \left[ \ln \left( \frac{8R}{g} \right) - 2 \right], \quad (22)$$

where  $\mu_0$  is the permeability of vacuum,  $R$  is the radius of the equivalent circuit (equals the distance between the center of the circuit and the wire axis), and  $g$  is the geometrical mean distance between the area of the wire cross section and itself. The geometrical mean distance is calculated by formula given in [3]

$$\ln(g) = \frac{1}{s_1 s_2} \iint_{s_1 s_2} \ln(\eta) ds_1 ds_2, \quad (23)$$

where  $\eta$  is the distance between the elementary areas  $ds_1$  and  $ds_2$ . The integration procedure is as follows: each of the variables  $ds_1$  and  $ds_2$  is integrated with respect to one another throughout the entire area and the procedure is repeated. If supposed that a high-frequency current flows in equivalent circuits and is uniformly distributed over the surface, then the geometrical mean distance for the stator turn circuits equals  $g_i = \frac{d}{2}$ ,  $d$  being the diameter of the stator turn wire [3]. For the armature rings and the metal cup rings, the logarithm of the geometrical mean distance between the area cross section and itself equals

$$\ln(g) = \ln(\xi + 0.0002) + \ln(0.2236), \quad (24)$$

where  $\xi$  is the width of the armature rings and the metal cup rings and 0.0002 is the depth  $\delta$  of the fixed skin-layer in meters (see Fig. 7).

The skin depth can be calculated for the given initial conditions: the HFCG design, and when heating is important the initial seed current is considered. For the solution stability of the system of HFCG equations, the skin depth is considered as a fixed value, and for  $\xi$  considerably larger than the skin depth, the approximation error is negligibly small. Account of the variations in the skin

depth has little effect on the value of the current derivative and only matters for HFCCGs with significantly varying mean operating frequency. Assuming that the symmetry axis of the circuit passes through the middle of the fixed skin depth one can eliminate the proximity effects of the stator wires from the consideration and suppose that the current is uniformly distributed over the surface of the stator turns.

The mutual inductance between two equivalent circuits of the stator turns is calculated as a mutual inductance between two infinitely thin circuits through a series representation [3]. The mutual inductance between the circuits of the rings of the armature and that between the circuits of the rings of the metal cup, as well as between the circuits of the armature ring or the metal cup ring and the stator turn is calculated from the geometrical mean distance.

### 7.1 Calculation of Mutual Inductance Between Equivalent Circuits from Geometrical Mean Distance

When the equivalent circuits of the armature and the cup, as well those of the armature rings and the stator turns are closely spaced, it is important that the geometrical dimensions of their cross sections be considered, which is achieved by taking account of the geometrical mean distance between the cross sections of the two circuits.

The mutual inductance between the equivalent circuits of the rings is calculated as a mutual inductance between two infinitely thin circuits, coinciding with the symmetry axes of the cross section of the current-carrying conductor. The distance between the circuits wires equals the geometrical mean distance between the cross sections of the two circuits (Fig. 7 and Fig. 8).

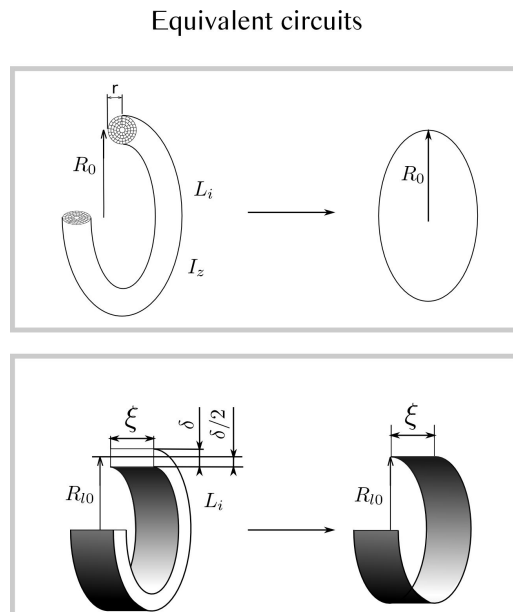


Figure 7: Equivalent circuits for mutual inductance calculation

The circuits of the armature rings and the metal cup rings are represented as the rings of an infinitely thin strip of width  $\xi$ . This approximation is correct for skin depths  $\delta$  considerably less than the width  $\xi$ .

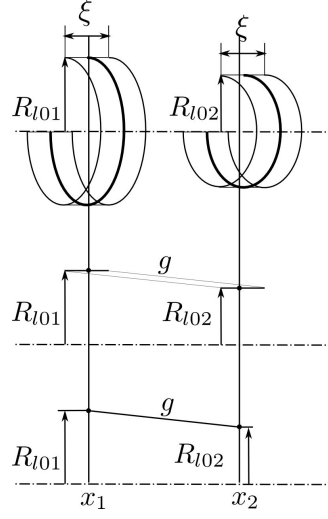


Figure 8: Calculation of mutual inductance between the circuits of the armature rings and the metal cup rings from geometrical mean distance

Thus, we calculate the geometrical mean distance between the cross sections of the armature rings and/or the metal cup rings (fig. 8). The mutual inductance of the circuits is taken equal to mutual inductance of two infinitely thin circuits whose radii are the same as the distance between the center of the ring and the symmetry axis of its cross section. The infinitely thin circuits are arranged so that the shortest distance between them is the same as the geometrical mean distance between the adjacent cross sections of the rings [3]. The geometrical mean distance between the cross sections of the armature rings and/or the metal cup rings is the geometrical mean distance between two segments (fig. 8). The geometrical mean distance between the cross sections of the stator turn and the armature rings or the metal cup rings is calculated as the geometrical mean distance between the point on the symmetry axis of the cross section of the stator turn and the segment of the cross section of the armature ring or the ring of the metal cup.

## 7.2 Decomposition of a Multiwire Stator with Symmetrical Wires into Current-Carrying Elements

The approach that we suggest is based on the decomposition of a stator formed by symmetrically arranged wires for the simplification of the computation procedure and reduction of errors in calculating the inductance of the stator. Let us make use of this fact that in the stator coil formed by several wires wound together and arranged symmetrically with each other, the same current passes through every wind due to symmetry.

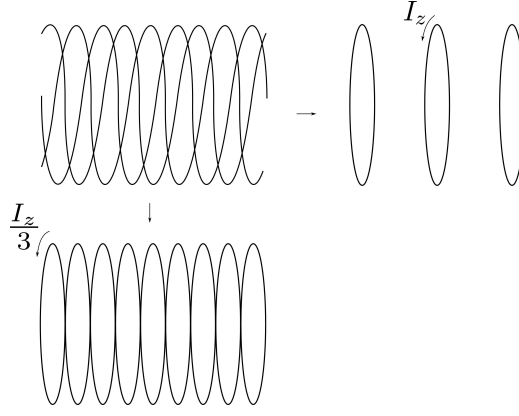


Figure 9: Decomposition of a multiwire stator with symmetrical wires

The stator turns are decomposed as follows: every wind has the same number of equivalent circuits as the number of winds. The dimensions of the equivalent circuits are assumed to be equal to the dimensions of the stator turn (the turn diameter and the wire diameter), as shown in Fig.9. In modeling HFCG operation, it should be taken into account in electrotechnical equations that the current passing through the obtained circuits is  $n$  times smaller than the current  $I_z$ . When the HFCG consists of the sections with different winds and wire diameters, every section is decomposed separately in consecutive order and is considered in the system of equations (13).

### 7.3 Decomposition of the Stator Turn into Parts of Equivalent Circuits and Computation of their Inductance in the Vicinity of a Moving Contact Point

Decomposition of the stator turns into equivalent circuits provides a helpful tool for describing the HFCG operation. At the final stage of HFCG operation, switching the circuit of the stator turn out of the stator-armature-load electric circuit leads to an appreciable change in the inductance of the HFCG stator, which result in a poorer modeling accuracy. For this reason, it is advisable that a more exact computation of the inductance be performed at the final stage of HFCG operation, when only several (ten or fewer) turns remain in the stator. The exact calculation of the stator inductance is performed by dividing the equivalent circuit of the stator turn into parts at the contact point. This is made for both a single wind and several symmetric winds. With this aim in view, one can use [3]:

$$M_{14} = \frac{1}{2} (L_{14} - L_1 - L_4), \quad (25)$$

where  $M_{14}$  is the mutual inductance of the two contacting parts of the wire that lie on the line curved along the circular arc;  $L_{14}$  is the inductance of the considered

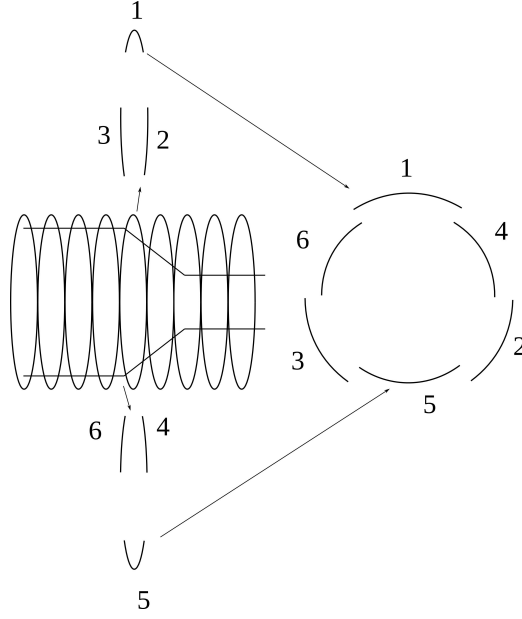


Figure 10: Decomposition of the stator in the vicinity of a moving contact point

segment of the arc 14;  $L_1$  and  $L_4$  and the inductances of its parts; and

$$M_{12} = \frac{1}{2} (L_{142} + L_4 - L_{14} - L_{42}), \quad (26)$$

where  $M_{12}$  is the mutual inductance of the two non-contacting parts of the wire that lie of the line curved along the circular arc;  $L_{142}$  is the inductance of the wire 142;  $L_4$  is the inductance of part 4;  $L_{14}$  is the combined inductance of parts 1 and 4; and  $L_{42}$  is the combined inductance of parts 4 and 2. The inductance of the wire composed of three parts is [3]

$$L = L_1 + L_4 + L_2 + 2(M_{14} + M_{42} + M_{21}), \quad (27)$$

where  $L$  is the inductance of part 142. The formula for calculating the self-inductance of the wire curved along the circular arc [3] reads:

$$L = Z - G + A - Q, \quad (28)$$

where  $Z$  depends only on the shape and size of the wire axis,  $G, A, Q$  depend on the wire cross section and the current distribution pattern over the cross section;  $G$  also being dependent on the length of the wire axis. If we neglected the quantities of the order of  $\frac{g}{2R_m}$  and  $\frac{g}{l}$  with  $l$  being the wire length and  $R_m$ , the least radius of curvature of the wire axis, then (28) can be written in the form:

$$L = Z - G \quad (29)$$

and

$$Z = \frac{\mu_0 R}{2\pi} \left[ \theta (\ln 8R - 2) - 4I' + 4 \sin \frac{\theta}{2} \right], \quad (30)$$



where  $\theta$  is the angle subtending the arc of length equal to the total length of the wire, while

$$I' = - \int_0^{\frac{\theta}{4}} \ln \tan \vartheta_1 d\vartheta_1, \quad (31)$$

and

$$G = \frac{\mu_0 l}{2\pi} \ln g. \quad (32)$$

Thus, using the contact point, it is possible to divide the equivalent circuit of the turn into parts and define their self- and mutual inductances.

The contact point divides the equivalent circuit of the turn of a single-wire stator into two parts, one of which is included into the common stator-armature-load electric circuit, while the other one is switched out of the circuit and is considered as a free circuit interacting with other circuits via the magnetic field (Fig. 10). Using the above formulas, let us calculate self-inductances of the parts of the turn and mutual inductances between them and other circuits.

By way of example, let us consider a three-wire stator; similar calculations for the case of a multiwire stator can be easily made by generalizing the above theorems and formulas. Because for symmetric winds of the stator we used the above-described method of division into the turns, the contact point divides the equivalent turns into number  $2n$  parts (Fig. 10).

Thus, using the above approach, one can define the self-inductance of a part of the stator turn bounded by a moving contact point (Fig. 10) in the stator-armature-load electric circuit as follows:

$$L = 3L_1 + 6M_{12}, \quad (33)$$

outside the circuit

$$L = 3L_4 + 6M_{45}. \quad (34)$$

The mutual inductance between the parts equals:

$$M = 3M_{15} + 6M_{14}. \quad (35)$$

## 7.4 Inductance of the Coaxial Part of the HFCG

It is important that in HFCG operation, the coaxial inductance of the stator that is associated with current  $I_z$  should be considered.

Though this inductance is small, it is vital to consider it at the final operation stage, when a few turns are left in the circuit, and small inductance values, which can be neglected at the initial stage, play an important role.

The projection of the current  $I_z$  on the HFCG axis is equal to itself (see a similar fluid flow problem in hydrodynamics). The stator is replaced by an equivalent

cylinder, with current  $I_z$  flowing along its axis (Fig. 11), which is furnished with a metal cup having a diameter approximately equal to the diameter of the equivalent cylinder. The cylinder wall is assumed to be infinitely thin, and the current density is uniformly distributed over its surface. The radius of the equivalent cylinder is assumed to be equal to the inner radius of the stator.

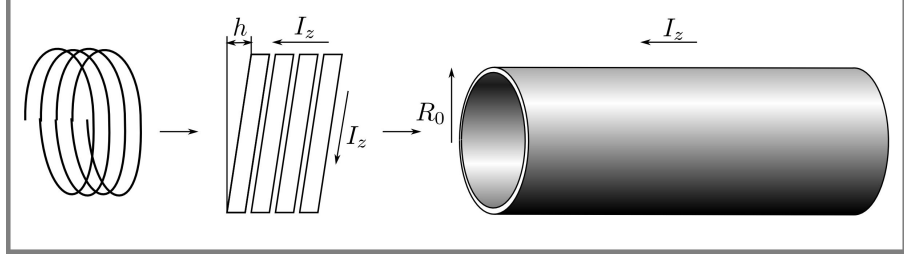


Figure 11: Inductance of the stator for the current projected on the HFCG axis

The self-inductance of the equivalent cylinder can be found in a similar manner as the inductance of a straight wire. Here the geometrical mean distance between the cross sections of the cylinder and itself equals its radius.

$$L = \frac{\mu_0 l}{2\pi} (\ln(\frac{2l}{r} - 1)), \quad (36)$$

where  $r$  and  $l$  are the radius and the length of the cylinder, respectively. The self-inductance of the armature is determined similarly.

It is possible to consider a stator with a liner in the form of a coaxial cable. In this case, the inductance of the HFCG part with a pipe-shaped armature and that of the HFCG part with a cone-shaped widening armature should be calculated separately.

$$L_l = L_k + L_m, \quad (37)$$

where  $L_k$  is the inductance of the HFCG with a cone-shaped armature and  $L_m$  is the inductance of the HFCG with a pipe-shaped armature; the HFCG part behind the contact point is dropped from the consideration.

The inductance for the current projection on the HFCG axis can be found with known magnetic flux:

$$L_{line}^z = \frac{1}{i^2} \int_s \Phi di, \quad (38)$$

where  $\Phi$  is the magnetic flux, which equals

$$\Phi = \int_S B dS. \quad (39)$$

Here  $B$  is the magnetic field inductance,  $S$  is the area of the closed current-carrying circuit with current  $i$ . Then we have

$$L_{line}^z = \frac{1}{i^2} \int_s \int_S B dS di. \quad (40)$$

When the symmetry of the coaxial part of the HFCG is taken into account, its inductance in cylindrical coordinates can be found by formula given in [6]

$$L_{line}^z = \frac{\mu_0}{2\pi} \int_0^l \int_{r_{arm}(z)}^{r_{stat}(z)} \frac{1}{r} dr dz, \quad (41)$$

where  $r_{arm}(z)$  is the radius of the armature,  $r_{stat}(z)$  is the radius of the stator,  $z$  is the length of the coaxial part of the HFCG.

## 8 Errors Related to Neglecting the Stator Helicity

When the stator helicity is taken into account, the current  $I_z$  can be decomposed into two components: along the OZ-axis, which is the generator's axis, and in the XY-plane. The projection of the current on the XY-plane equals the current  $I_z$  and so does its projection on the OZ-axis.

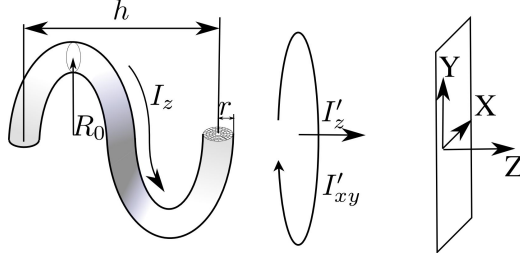


Figure 12: Decomposition of the current  $I_z$  into the current azimuthal along the OZ-axis (the HFCG axis) and the current in the XY-plane

Neglecting the stator helicity, one can readily find the inductance of the turn in the XY-plane by formula (22).

Let us evaluate the helicity effect on the calculations of the stator inductance. For the case of uniform distribution of the current density over the wire cross section, the formula for calculating the self-inductance can be written as follows:

$$L = \frac{1}{s^2} \iint_{s_1 s_2} \overline{M}_k ds_1 ds_2, \quad (42)$$

where

$$\overline{M} = \frac{\mu_0}{4\pi} \iint \frac{dl_1 dl_2 \cos \theta}{D}. \quad (43)$$

Here it is assumed that  $\theta$  is the angle between the length elements  $dl_1$  and  $dl_2$  in the XY-plane. For rings

$$D = 2R \sin \frac{\theta}{2}, \quad (44)$$

with due account of the helicity

$$D = \sqrt{\left(2R \sin \frac{\theta}{2}\right)^2 + \left(\frac{h}{2\pi} \theta\right)^2}, \quad (45)$$

where  $h$  is the coil pitch.

Disregarding the helicity of the stator in finding the mutual inductance between the stator turns, we have

$$D = \sqrt{\left(2R \sin \frac{\theta}{2}\right)^2 + (nh)^2}, \quad (46)$$

where  $n = |i - j|$  and  $nh$  is the distance between the centers of the turns  $i$  and  $j$  when the coil pinch is constant.

When the helicity is taken into account, we have:

$$D = \sqrt{\left(2R \sin \frac{\theta}{2}\right)^2 + (nh)^2 + \left(\frac{h}{2\pi}\theta\right)^2}; \quad \frac{\theta}{2\pi} \leq 1. \quad (47)$$

From the above formulas follows that when the effect of the stator helicity on the self-inductance of the turn is strong, this effect should be checked against the difference between the self-inductance of the ring and the turn having a pitch  $h$ , which enables one to check the approximation accuracy when the turns are replaced by the rings.

## 9 Resistance

### 9.1 Skin Layer

The skin-layer technique is the most common method for calculating the HFCG resistance. This method is based on the assumption that the total current uniformly flows through the plate of thickness equal to the skin depth (see Fig. 13). The skin depth  $\delta$  can be found by formula

$$\frac{\rho}{\delta} = k \sqrt{\frac{dI(t)}{dt} I(t)}, \quad (48)$$

where  $\rho$  is the specific resistance ( $1.72 \cdot 10^{-8}$  copper) and  $k = \sqrt{\mu_0 \rho}$  is the coefficient, which for copper equals  $1.47 \cdot 10^{-7}$ . The resistance of the circuit is defined by the formula for the resistance of the ring:

$$R = \frac{2\pi r \rho (1 + \alpha_T T)}{d \delta}, \quad (49)$$

where  $r$  is the radius of the circuit,  $d$  is the wire diameter (metal),  $\alpha_T$  is the temperature coefficient (0.0043 for copper), and  $T$  is the temperature (it always equals zero when heating is ignored)

A similar resistance model for the circuits of the armature ring and the metal cup ring is defined by:

$$R = \frac{2\pi r \rho (1 + \alpha_T T)}{\delta \cdot \xi}, \quad (50)$$

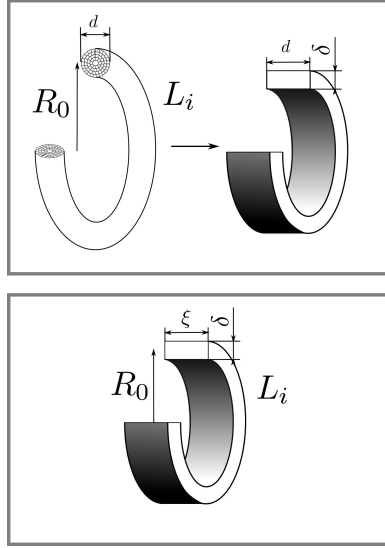


Figure 13: The schematic representation of the resistance calculations using the skin-layer technique

where  $\xi$  is the width of the armature ring and the metal cup ring (in the general case, they can differ).

To find the resistance  $R_{line}$  of the armature and the metal cup to current  $I_z$ , let us add together the corresponding resistances of the armature rings and the metal cup rings to the current flowing in the direction of the OZ-axis:

$$R_{line} = \frac{\xi \cdot \rho(1 + \alpha_T T)}{\pi(d\delta + \delta^2)}, \quad (51)$$

where  $\pi(d\delta + \delta^2)$  corresponds to the area of the ring of radius  $r$  and the width  $\delta$ .

## 9.2 Nonlinear Magnetic Diffusion

In this subsection, we have found the HFCCG resistance from depth distribution of the current density in the stator turns and the armature rings. The current density distribution was determined from the equations for nonlinear magnetic diffusion into an infinite conducting plate [4]:

$$\frac{\partial H_z}{\partial x} = -\frac{1}{\rho_0(1 + \beta Q)} E_y = -j, \quad (52)$$

$$\frac{\partial E_y}{\partial x} = -\mu_0 \frac{\partial H_z}{\partial t}, \quad (53)$$

$$\frac{\partial Q}{\partial t} = (1 + \beta Q) \rho_0 \left( \frac{\partial H_z}{\partial x} \right)^2. \quad (54)$$

The initial conditions are as follows:

$$\begin{aligned} x = 0 : H_z(0, t) &= H_0(t), t \geq 0, \\ t = 0 : H_z(x, 0) &= 0, x \geq 0. \end{aligned}$$

Rewrite (54) using (52)

$$\frac{\partial Q}{\partial t} = (1 + \beta Q)\rho_0 j^2, \quad (55)$$

and (53) using (52)

$$\frac{\partial(\rho_0(1 + \beta Q)j)}{\partial x} = -\mu_0 \frac{\partial H_z}{\partial t}. \quad (56)$$

Let us write a more detailed expression for a partial derivative:

$$j\beta\rho_0 \frac{\partial Q}{\partial x} + \rho_0(1 + \beta Q) \frac{\partial j}{\partial x} = -\mu_0 \frac{\partial H_z}{\partial t}. \quad (57)$$

Here the initial and final conditions are as follows:  $x = 0 : \frac{\partial H_z(0, t)}{\partial t} = f(t), t \geq 0$ ;  
 $t = 0 : H_z(x, 0) = 0, j(x, 0) = 0, Q(x, 0) = 0, x \geq 0$ .

Let us take a flat plate of thickness  $\frac{d}{2}$  and width  $d$  (Fig. 14), but we shall consider that the magnetic field is diffused into the infinite plate of finite thickness.

In the absence of an external magnetic field, the magnetic field strength near the plate surface is [5]:

$$H = \frac{i}{2}, \quad (58)$$

where  $i$  is the surface current density. The partial time derivative is

$$\frac{\partial H}{\partial t} = \frac{1}{2} \frac{\partial i}{\partial t}. \quad (59)$$

Let  $H_0$  denote the magnetic field strength in front of the plate in the case of an external magnetic field when a zero total magnetic field behind the plate

$$H_0 = i. \quad (60)$$

Take a time partial derivative

$$\frac{\partial H_0}{\partial t} = \frac{\partial i}{\partial t}. \quad (61)$$

Divide the plate into  $n$  number layers of thickness  $h_x$  (Fig. 14).

The time derivatives of the magnetic field strength in the adjacent layers of the plate are related as follows:

$$\frac{\partial H_k}{\partial t} = \frac{\partial H_0}{\partial t} - \int_0^{x_k} \frac{\partial j_k}{\partial t} dx \approx \frac{\partial H_0}{\partial t} - h_x \sum_{p=1}^k \frac{\partial j_p}{\partial t}. \quad (62)$$

Define the boundary condition on the plate surface as

$$\frac{\partial H_0}{\partial t} = \frac{1}{d} \frac{\partial I}{\partial t}, \quad (63)$$

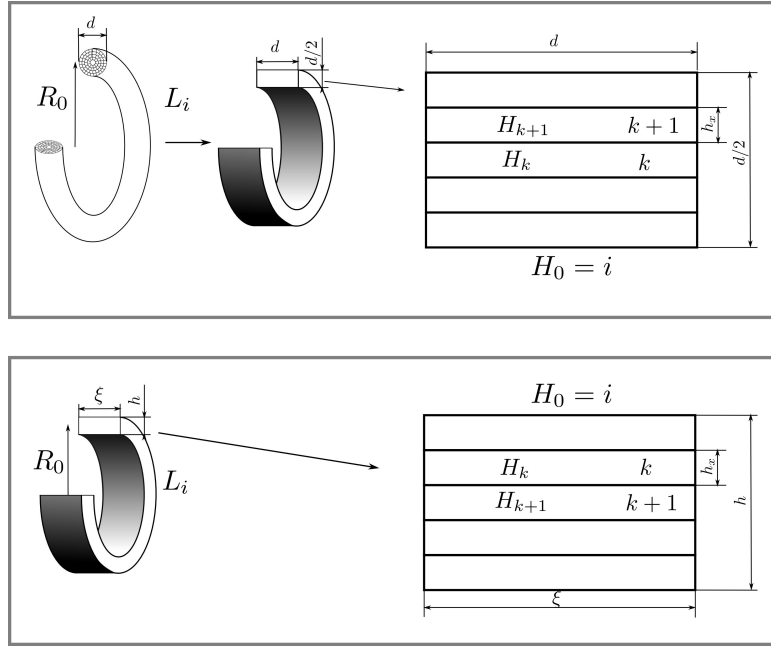


Figure 14: Schematic representation of the plate division

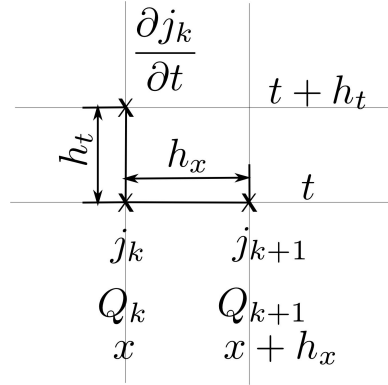


Figure 15: Difference scheme

where  $\frac{\partial I}{\partial t}$ , the current derivative in the equivalent circuit, is given in the computer code for HFCG calculations. The formula for the difference scheme can be written in the form:

$$\rho_0 \beta j_{k+1} \frac{Q_{k+1} - Q_k}{h_x} + \rho_0 (1 + \beta Q_{k+1}) \frac{j_{k+1} - j_k}{h_x} = -\mu_0 \left( \frac{\partial H_0}{\partial t} - h_x \sum_{p=1}^k \frac{\partial j_p}{\partial t} \right). \quad (64)$$

From this one can find  $\frac{\partial j_k}{\partial t}$  for  $k = \overline{1..n-1}$  and determine the nod values of current density in the next time step. For  $k = n$

$$\frac{\partial j_k}{\partial t} h_x = \frac{\partial H_0}{\partial t} - h_x \sum_{p=1}^{n-1} \frac{\partial j_p}{\partial t}. \quad (65)$$

Since this difference scheme exhibits poor convergence and requires the use of very small integration steps, for the above formulas we shall write the difference

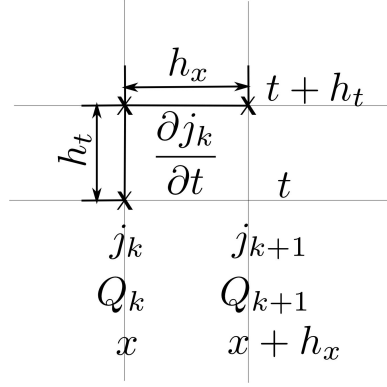


Figure 16: The difference scheme for the implicit Euler method

scheme for the implicit Euler method:

$$\rho_0 \beta j_{k+1}^{t+h_t} \frac{Q_{k+1}^t - Q_k^t}{h_x} + \rho_0 (1 + \beta Q_{k+1}^t) \frac{j_{k+1}^{t+h_t} - j_k^{t+h_t}}{h_x} = -\mu_0 \left( \frac{\partial H_0}{\partial t} - h_x \sum_{p=1}^k \frac{j_p^{t+h_t} - j_p^t}{h_t} \right). \quad (66)$$

Upon multiplying by  $\frac{h_t}{\mu_0 h_x}$  and transposing the terms containing the current density of the time step  $t + h_t$ , the left-hand side of (66) takes the form:

$$\frac{h_t}{\mu_0 h_x} \rho_0 \beta j_{k+1}^{t+h_t} \frac{Q_{k+1}^t - Q_k^t}{h_x} + \frac{h_t}{\mu_0 h_x} \rho_0 (1 + \beta Q_{k+1}^t) \frac{j_{k+1}^{t+h_t} - j_k^{t+h_t}}{h_x} - \sum_{p=1}^k j_p^{t+h_t}. \quad (67)$$

On the right-hand side of (66), we have:

$$- \frac{h_t}{h_x} \frac{\partial H_0}{\partial t} - \sum_{p=1}^k j_p^t. \quad (68)$$

The difference scheme for the implicit Euler method is given in Fig. 16. Solving the obtained system of inhomogeneous linear equations, one can find the current density derivatives in each layer of the plate. Let us estimate the resistance. The formulas used in electric engineering for calculating resistance in parallel conductors are not applicable because they require determining the resistance which occurs in the plate layers due to the magnetic field change. The active resistance describes dissipative processes in the system, hence the resistance in the circuit can be determined with known energy losses. Then for the general case, we can write:

$$Q_{total}^{t+h_t} - Q_{total}^t = RI^2 h_t = \sum_{k=1}^n \left( Q_{k,total}^{t+h_t} - Q_{k,total}^t \right), \quad (69)$$

where  $Q_{total}^t$  is the electromagnetic field energy that has passed through the conductor during time  $t$ ,  $h_t$  is the integration time step, and  $k$  is the subscript num-



bering the plates in the ring

$$R = \frac{\sum_{k=1}^n (Q_{k,total}^{t+h_t} - Q_{k,total}^t)}{I^2 h_t}. \quad (70)$$

In the integral representation of the energy equation [4] two types of field losses are distinguished:

$$- \int_S \mathbf{P} ds = \int_V \frac{\partial}{\partial t} (Q + W) dV, \quad (71)$$

where  $\frac{\partial Q}{\partial t} = \rho j^2$  is the Joule loss,  $j$  is the current density,  $\frac{\partial W}{\partial t} = \mathbf{H} \frac{\partial \mathbf{B}}{\partial t} = \frac{\partial}{\partial t} (\frac{1}{2} \mu \mathbf{H}^2)$  is the change of the electromagnetic field energy, and  $\mathbf{P} = (\mathbf{E} \times \mathbf{H})$  is the Poynting vector, i.e, the energy flux passing through the surface.

Express the derivative of the magnetic field energy in terms of the surface current density:

$$\frac{\partial W}{\partial t} = \mathbf{H} \frac{\partial \mathbf{B}}{\partial t} = i \mu \frac{\partial i}{\partial t}. \quad (72)$$

For each plate layer with the current, we can write

$$\frac{W_k^{t+h_t} - W_k^t}{h_t} = \mathbf{H}_k \frac{\partial \mathbf{B}_k}{\partial t} = i_k \mu \frac{\partial i_k}{\partial t}. \quad (73)$$

Using (55), let us find the energy released through Joule heating

$$Q_k^{t+h_t} = Q_k^t + \int_t^{t+h_t} (1 + \beta Q_k^t) \rho_0 (j_k^t)^2 dt. \quad (74)$$

Application of Simpson's rule for numerical integration gives

$$Q_k^{t+h_t} = Q_k^t + (1 + \beta Q_k^t) \rho_0 h_t \left( (j_k^t)^2 + 4 \left( j_k^t + \frac{\partial j_k^{t+h_t}}{\partial t} \frac{h_t}{2} \right)^2 + \left( j_k^t + \frac{\partial j_k^{t+h_t}}{\partial t} h_t \right)^2 \right) / 6. \quad (75)$$

Finally, we have for the resistance:

$$R = \frac{\sum_{k=1}^n (Q_k^{t+h_t} - Q_k^t + W_k^{t+h_t} - W_k^t)}{I^2 h_t}. \quad (76)$$

The obtained formula shows that the heating losses can be determined from the current density distribution. When the resistance is found from the skin depth, the losses related to the diffusion of the magnetic field into the conductor should be included along with the Joule losses. Thus, the accurate calculation of heating and temperature values seems to be more complicated.

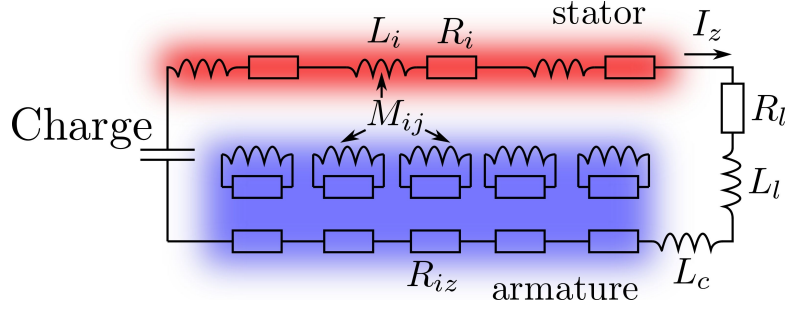


Figure 17: Electrotechnical scheme of the proposed 2D model

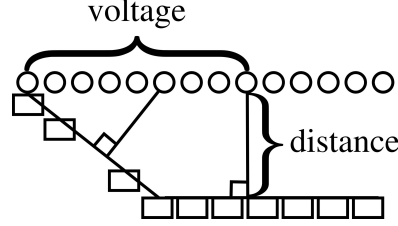


Figure 18: HFCG electric field strength calculation

## 10 Voltage and Electric Field Strength in the HFCG

Upon calculating  $U_i$  from the system of equations (13), one can find the voltage across each equivalent circuit of the stator turn. As is seen from the schematic diagram of the HFCG (Fig. 17), summation of the voltages across the turns with respect to the armature gives the stator-armature voltage over the HFCG length. The voltage produced by the current  $I_z$  in the armature can be neglected because it only amounts to several per cent of the voltage across a single turn, being as small as the calculation error for the voltage across the turns in the vicinity of the contact point in a two-dimensional model. With known voltage across the stator turns, one can make a map of the electric field strength for the stator-liner field upon calculating the distance between the wires of the turns. This distance is determined with regard for the size of the wire and the position of the liner at each instant of time Fig. 18.

## 11 The Model of HFCG Seeding. Plastic and Metal Cups.

Seed sources of different types are used for feeding the HFCG: capacitor banks, storage batteries, and other HFCGs. We shall consider the option where a capacitor bank is used as a seed source for its simplicity. The capacitor bank is charged first and then discharged into the HFCG via the connectors, thus causing the current gain in the HFCG. After high explosives are ignited, the stator or the metal cup is connected to the armature, the HFCG operates independently of the capacitor bank.

Let us distinguish two HFCG designs according as a metal or plastic cup is

used. For the case of a metal cup with the length comparable to the diameter of the stator, the armature gets connected to the metal cup far from the stator, and the derivative of the HFCG inductance is less than the losses in the circuit, so the current decreases. The current starts to increase when the vertex of the armature cone reaches the stator.

From the viewpoint of electrical technology, the case when a plastic cup is used is similar to that without a metal cup. The stator is connected to the armature at the first turn. It occurs at the moment when feeding from the capacitor bank is stopped, and the bank continues feeding the HFCG until the armature is connected to the stator. The HFCG inductance changes during the seeding process, and the current derivative is usually positive (of the same sign). In this case, there is an option of whether to calculate the HFCG inductance from the magnetic flux or from the magnetic energy. These methods give different results for the derivative of the HFCG inductance, and the difference is most significant during the seeding process. For this reason, an accurate model of the process of seeding the HFCG with a plastic or a metal cup would enable one to choose a more appropriate method of the two, thus demonstrating its advantages.

## 12 Conclusion

This paper describes a two-dimensional model of a helical FCG, based primarily on fundamental physical principles. The experimental results have been described for various HFCG designs and operation parameters with an accuracy within instrumental error. The idea stated in [7] that the intrinsic losses in the magnetic flux are not of resistive character has been confirmed and the physical explanation for these losses has been suggested, as well as the method of their calculation. The model of nonlinear diffusion of the magnetic field into the conductor and the model of resistance have been developed. It has been shown that the magnetic field diffusing into the conductor is the source of magnetic flux losses, which enhance the resistance of the conductor, and the resulting resistance equals the resistance of the conductor calculated using the skin-depth technique. It has also been demonstrated that the method of elimination of the stator turns from the system of equations (7), (9) and re-calculation of the current in the turn is redundant. The proposed model of the moving contact point enables one to demonstrate the mechanism of the intrinsic flux losses and present a physically correct two-dimensional model of a helical FCG for the description and anticipation of experimental results.

However, some processes in a two-dimensional model are simplified, thus limiting its application, for example, for the description of an HFCG whose stator coil has widely-spaced turns with inter-turn spacing comparable to the diameter of the

coil wire. In this case, one should use a three-dimensional HFCG model, which correctly accounts for the current density distribution over the wire cross section. It should be noted that the resistance of the stator turns can differ as much as by a factor of three, depending on the distance to the contact point, though the average resistance of the turns is practically constant, which follows from the problems solved in a 3D model [12]. Development of a valid three-dimensional model for HFCG description is the next step in theoretical analysis of HFCGs.

## References

- [1] Sakharov A. D. et al. Sov. Phys. Dokl. 10 1045 (1966)
- [2] Fortov V. E. Explosive-driven Generators of Powerful Electric Current Pulses Cambridge International Science Publishing, 2003
- [3] Kalantarov P. L. and Zeitlin L. A. Calculation of Inductances: A Handbook, Leningrad, Energoatomizdat, 1986 (in Russian).
- [4] Knoepfel H. Pulsed High Magnetic Fields, North-Holland, Amsterdam 1977.
- [5] Kingsep A. S., Lokshin G. R. and Ol'khov O. A., Fundamentals of Physics. Physics in 2 v. V. 1. Mechanics, Electricity and Magnetism, Waves, wave optika.uchebnik for universities. FIZMATLIT, 2001(in Russian).
- [6] B.M. Novac, I.R. Smith, M.C. Enache, H.R. Stewardsom Simple 2D model for helical flux-compression generators, Laser and Particle Beams (1997), vol. 15 , no3, pp. 379-395
- [7] Neuber A. A. (editor) Explosively Driven Pulsed Power: Helical Magnetic Flux Compression Generators, Springer, Berlin, 2005. P. 280.
- [8] G. F. Kiuttu and J. B. Chase, An armature-stator contact resistance model for explosively driven helical magnetic flux compression generators, Proc. 15th IEEE Intl. Pulsed Power Conf., Monterey (2005).
- [9] G.F. Kiuttu, J.B. Chase, D.M. Chato, G.G. Peterson Recent advances in modeling helical FCGs Proceedings of Megagauss XI, Santa Fe, Omnipress, pp. 255 264 (2008).
- [10] J.C. Crawford and R.A Damerow, Explosively Driven High-Energy Generators, J. Appl. Phys., 39, No. 11, pp. 5224-5231 (1968).
- [11] Fowler C.M., Garn W.B. and Caird R.S. Production of very high magnetic fields by implosion, J.Appl.Phys. 1960. V. 31. P. 588594.

- [12] Haurylavets V.V. and Tikhomirov V.V, 3-D modeling for losses in HF CGs, International student's forum "First step in science - 2009", Minsk, Pravo i ekonomika, 2010, v.2, p.630 (in Russian).
- [13] Paul, Clayton R Inductance: Loop and partial / by Clayton R Paul.– New Jersey: Wiley-IEEE Press, 2010. xiii, 379p. ISBN : 9780470461884. 621.3742 P10 185367